Soil Biology and Biochemistry 180 (2023) 108991

Contents lists available at ScienceDirect

Soil Biology and Biochemistry

journal homepage: www.elsevier.com/locate/soilbio

Greater regulation of permafrost organic matter composition by enzymes and redox than temperature

Laurel Lynch [a,*], Andrew Margenot [b], Francisco Calderon [c], Jessica Ernakovich [d]

[a] Department of Soil and Water Systems, College of Agricultural and Life Sciences, University of Idaho, Moscow, ID, 83844, USA
[b] Department of Crop Sciences, College of Agricultural, Consumer, and Environmental Sciences, University of Illinois Urbana-Champaign, Urbana, IL, USA
[c] Columbia Basin Agricultural Research Center, College of Agricultural Sciences, Oregon State University, Adams, OR, 97801, USA
[d] Department of Natural Resources and the Environment, College of Agricultural and Life Sciences, University of New Hampshire, Durham, NH, 03824, USA

ARTICLE INFO

Keywords:
Permafrost chemistry
Fourier transform infrared (FTIR) spectroscopy
Extracellular enzyme activities
Redox

ABSTRACT

Accelerating permafrost thaw across high-latitude ecosystems increases organic matter (OM) availability to soil microorganisms. The chemical composition of permafrost-derived OM, which influences microbial metabolic efficiency, may determine whether the Arctic remains a critical carbon sink in the future or shifts to net a source of greenhouse gases. During a 90-day, simulated thaw experiment, we measured shifts in the chemistry of soil and dissolved organic matter pools sourced from surface (0–10 cm) and subsurface (16–25 cm) permafrost layers. We manipulated temperature (1 versus 15 °C) and redox (drained versus saturated) to mimic field-relevant conditions and tested whether variability in OM chemistry could be explained by the activities of six hydrolytic enzymes that catalyze carbon, nitrogen, and phosphorus mineralization. We found that permafrost depth and enzyme activities were significantly correlated with shifts in soil OM (SOM) functional group chemistries, as measured by diffuse reflectance infrared Fourier transform (DRIFT) spectroscopy. Greater variability in dissolved OM (DOM) chemistries were driven by redox and pH. Our results suggest depth-resolved analyses of permafrost vulnerability to enzymatic hydrolysis may help explain distinct patterns in SOM versus DOM cycling that can be used to constrain modeled projections of Arctic carbon storage during global change.

1. Introduction

Nearly one-quarter of the terrestrial Northern Hemisphere is underlain by permafrost (Zhang et al., 1999), which stores twice as much carbon (C) as the pre-industrial atmosphere (Hugelius et al., 2014). The longevity of this historically stable C sink is increasingly threatened by anthropogenic climate change (French and Slaymaker, 2011; Koven et al., 2013; Romanovsky et al., 2010; Slater and Lawrence, 2013) as Arctic air temperatures are rising nearly four times faster than the global mean (Rantanen et al., 2022). Complex biological feedbacks make it difficult to predict whether greater permafrost thaw (Romanovsky et al., 2010) will induce a positive permafrost C-climate feedback. However, an ensemble of 50 models converge in their projection that every 1 °C of global warming could release 3–41 Pg C by the year 2100 from northern latitude regions (Biskaborn et al., 2015), suggesting enhanced decomposition will drive significant soil C losses.

The magnitude, rate, and form of C loss following permafrost thaw depends on many factors. For example, microtopographical variation across landscape position influences temperature and redox potentials (Ernakovich et al., 2017; Walz et al., 2017), the chemical composition of organic matter (Hodgkins et al., 2014; Schädel et al., 2014; Sjögersten et al., 2016), and the functional potential of microbial decomposers (Dohnalkova et al., 2017; Knoblauch et al., 2018; McCalley et al., 2014; Perryman et al., 2022), which collectively govern mineralization rates. Results from a 100-year simulated thaw found that permafrost C concentrations decreased by 75% when soils freely drained, but by only 9% when soils remained saturated (Elberling et al., 2013). Others found that stable CH_4-producing anaerobic microbial communities liberated more CO_2–C equivalents from permafrost thawed under anoxic than oxic conditions (Knoblauch et al., 2018). There is substantial evidence that permafrost chemistries vary by depth (Ernakovich et al., 2015), but it remains unclear how variable chemistries will influence mineralization rates. Across a 40-year-old permafrost thaw gradient in Sweden, Hodgkins et al. (2014) observed a strong association between the chemical composition of organic matter and C losses as CO_2 and CH_4 emissions, while others found that differences in chemistry between

* Corresponding author. Department of Soil and Water Systems, University of Idaho Moscow, 875 Perimeter Dr, ID, 83844, USA.
E-mail address: llynch@uidaho.edu (L. Lynch).

https://doi.org/10.1016/j.soilbio.2023.108991
Received 27 October 2022; Received in revised form 17 January 2023; Accepted 22 February 2023
Available online 22 February 2023
0038-0717/

active layer and permafrost soil horizons did not translate to differences in mineralization rates (Ward and Cory, 2015). Further investigation is therefore required to unravel how temperature, redox conditions, microbial activity, and permafrost chemistry interactively govern vertically-stratified decomposition rates and greenhouse gas emissions (Ernakovich et al., 2017).

Soil organic matter (SOM) persistence is partially regulated by enzyme kinetics and temperature (Schimel and Weintraub, 2003; Trivedi et al., 2016). Temperature regulates the rates at which soil hydrolytic enzymes catalyze SOM decomposition via depolymerization (Nannipieri et al., 2018; Wallenstein et al., 2009, 2010). As a result, permafrost thaw may increase rates of enzyme catalysis independent of the amount and timing of enzyme secretion by soil microorganisms (Kleber, 2010). Indeed, seasonal fluxes of dissolved organic matter (DOM) in peatlands have been attributed to temperature-driven changes in enzyme activities (Fenner et al., 2005). As a result, there is considerable interest in incorporating enzyme activities into assessments of SOM change during permafrost thaw to improve model predictions of temperature and redox changes on mineralization (Allison et al., 2010; Chen et al., 2016).

The release and decomposition of permafrost OM has implications for C storage and loss beyond the pedon scale. Dissolved organic matter serves as a critical intermediary pool in the global C cycle (Battin et al., 2009; Von Freyberg et al., 2014) because it is composed of reactive, low molecular weight compounds that fuel microbial metabolism (Kalbitz et al., 2003; Kellerman et al., 2014; Lynch et al., 2019b). The mobilization of DOM through Arctic watersheds links surface to subsurface soil horizons and energy flows across the terrestrial-aquatic interface (Lynch et al., 2019a; Zhang et al., 2017). As microbial communities encounter novel forms of DOM released from successively deeper permafrost thaw layers, substrate use efficiencies and enzyme cascades will likely determine whether DOM primes SOM decomposition (Fontaine et al., 2007; Keuper et al., 2020; Wild et al., 2014), catalyzing a positive feedback on C loss from thawing permafrost (Dutta et al., 2006; Schaefer et al., 2011; Schmidt et al., 2011), or promotes microbial anabolism and the physicochemical retention of microbial-derived C on freshly exposed soil minerals (Liang et al., 2017; Miltner et al., 2012). The interplay between permafrost chemistry and soil enzyme activity may therefore be a critical, yet overlooked, pathway in determining the trajectory and fate of Arctic C stocks (Heslop et al., 2021; Trivedi et al., 2016).

Here, we combine diffuse reflectance infrared Fourier transform (DRIFT) spectroscopy with assays of hydrolytic enzyme activities to monitor shifts in SOM and DOM composition during permafrost thaw. DRIFT spectroscopy measures the absorbance of infrared-active (i.e., polar) bonds and is sensitive to minor changes in organic functional group composition (Artz et al., 2008; Calderón et al., 2013). DRIFT spectroscopy is particularly useful to evaluate permafrost OM composition, given relatively low mineral content (Ernakovich et al., 2015; Hodgkins et al., 2014; Matamala et al., 2017), and to shifts in DOM composition during decomposition (Ernakovich et al., 2017). Spectroscopic analysis of Arctic DOM has helped elucidate the role particular C chemistries play as SOM is decomposed and mineralized. For example, DRIFT absorbances of DOM revealed changes in the relative abundance of specific organic functional groups (e.g., polysaccharides C–O, aliphatic C–H) due to anoxia under mesocosm incubations and improved modeled prediction of CO_2 and CH_4 emissions during permafrost thaw and mineralization (Ernakovich et al., 2017).

The objective of this study was to determine how simulated permafrost thaw influences biological feedbacks on permafrost chemistry. Using a 90-day thaw experiment to represent the average length of one growing season, we varied saturation (drained, saturated) and temperature (1 or 15 °C) conditions and evaluated shifts in bulk SOM and drained DOM chemistries. While we previously observed changes in DOM between soils undergoing aerobic and anaerobic metabolism in laboratory mesocosms (Ernakovich et al., 2017), we hypothesized that bulk SOM chemistry would be less sensitive to the different incubation conditions over this timescale than DOM. Additionally, because extracellular soil enzymes act upon organic matter bonds detectable by DRIFT spectroscopy (e.g., polysaccharide C–O), we hypothesized that hydrolytic soil enzymes would explain variation in SOM and DOM functional groups among thaw treatments. Specifically, we evaluated three questions.

(1) How does the interplay of permafrost depth, temperature, and redox influence bulk SOM versus DOM composition during simulated thaw?
(2) Does SOM composition predict the chemical composition of DOM released during thaw?
(3) To what extent can hydrolytic soil enzyme activities explain observed changes in organic matter functional groups under varying thaw conditions?

2. Methods

2.1. Site description and sampling

Permafrost samples were collected from under moist acidic tundra vegetation at Sagwon Hills, Alaska in August 2009 (N 69° 25′ 32.190″ W 148° 41′ 38.731″, 288 m above sea level). Borden et al. (2010) and Ernakovich et al. (2015) previously described site and soil characteristics. Soils developed from loess over gravel and are classified as Ruptic Histic Aquiturbels (Borden et al., 2010). The active layer depth at the time of sampling was 26.8 ± 1.3 cm. Permafrost layers were sampled from 0 to 10 and 16–25 cm below the frozen surface; permafrost depths from the soil surface were thus 27–37 cm and 43–52 cm. After removing the active layer, permafrost soils were sampled as cores using a Tanaka auger with a SIPRE-style soil corer with carbide bits (Jon's Machine Shop, Fairbanks, AK, (Tarnocai and Smith, 1993). Soils were homogenized to 4-mm sieve size while frozen as described in Ernakovich et al. (2015).

2.2. Incubation

Permafrost samples were subjected to either oxic or anoxic incubation conditions (referred to as the redox treatment) at two different temperatures (1 or 15 °C, referred to as the temperature treatment) as previously described (Ernakovich et al., 2017). Soil cores were randomly assigned to either the oxic or anoxic condition, such that soils from both the 0–10 and 16–25 cm depth were included in the same treatment. Soil samples were then divided into halves for incubation at 1 and 15 °C. There was a total of six replicates for each redox-temperature combination at each depth (n = 132 samples total). Soils were incubated in 473 ml plastic containers (Silgan Plastics Corporation, Norcross, GA) inside 1.89 L glass jars with gas-tight metal lids fitted with two septa ports. Samples assigned to the oxic treatment were allowed to drain through holes drilled in the plastic containers as they thawed, while samples in the anoxic treatment remained inundated. Drained water was removed from the oxic treatment jars after 5 days of thaw for the 15 °C treatment and 10 days of thaw for the 1 °C treatment. Glass jars in the anoxic treatment were never opened during the incubation. As described by Ernakovich et al. (2017), headspace atmosphere was replaced regularly throughout the 90-day incubation through the two septa ports by flushing the jars with either N_2 gas or CO_2-free air for the anoxic and oxic treatments, respectively. At the end of the experiment, soil redox was measured using a VWR sympHony epoxy combination redox electrode probe and Thermo Scientific Orion 3 Star meter (Ernakovich et al., 2017). Redox values for the oxic (339.77 ± 8.17 mV) and anoxic (240.45 ± 53.60 mV) treatments differed ($p < 0.05$), but the average for both fell within the denitrification range (Seo and DeLaune, 2010) despite significant differences in the CO_2:CH_4 ratio (Ernakovich et al., 2017). Thus, we hereafter refer to oxic treatments as 'drained' and anoxic treatments as 'saturated'.

Porewater DOM was collected at the end of the 90-day thaw by spinning 10 g of homogenized soil for 30 min at 580×*g* through pre-conditioned 0.45 μm nylon spin filters (Grace Discovery, Bannockburn, IL). Filters were pre-conditioned by spinning them three times with 9 ml of deionized (DI) water for 5 min at 580×*g*. Porewater samples were frozen for approximately 1 month at −20 °C and then analyzed for C and N content on a total organic carbon analyzer (Shimadzu Scientific Instruments, Inc.), with detection limits of 4 μg L^{-1} for TOC and 5 μg L^{-1} for TDN.

2.3. DRIFT spectroscopy

2.3.1. Bulk SOM

Pre- and post-incubation soils were analyzed by DRIFT spectroscopy in the mid-infrared region (4000–400 cm^{-1}) using Digilab FTS 7000 Fourier transform spectrometer (Varian, Inc., Palo Alto, CA with a deuterated, triglycine sulfate detector (DTGS) and a potassium bromide (KBr) beam splitter. The spectrometer was fitted with a Pike AutoDIFF diffuse reflectance accessory (Pike Technologies, Madison, WI). Background spectra were collected on KBr and soil spectra were collected using ground, air-dried, neat (no KBr dilution) soil samples. The use of neat soils, rather than KBr diluted samples, can enhance organic absorbances (Margenot et al., 2017a; Nguyen et al., 1991) and therefore increase sensitivity to organic functional groups. Data were obtained as pseudo-absorbance (log [1/reflectance]). Spectra were collected in duplicate on separate soil sub-samples at 4 cm^{-1} resolution for 64 co-added scans. Spectra were mean-centered and pretreated with multiplicative scatter correction prior to averaging duplicate spectra. The resulting mean spectra were used for all additional analyses.

To enhance absorbance of organic functional groups, spectra were mathematically treated by spectral subtraction to reduce mineral interferences (Margenot et al., 2015). To provide a mineral-enriched background spectrum for subtractions, permafrost samples were treated with sodium hypochlorite to remove OM based on the method of Anderson (1961) as described by Ernakovich et al. (2015). This method was selected to remove OM because it has minimal effects on mineral bands and particle size relative to other methods such as ashing (Margenot et al., 2017a). In our study, sodium hypochlorite oxidation removed 83% of C in the 0–10 cm layer (11.0 mg C g^{-1} remaining) and 90% of C in the 16–24 cm layer (4.5 mg C g^{-1} remaining). To minimize mineral bands while enhancing organic bands, the subtraction factor was adjusted (1.20–1.02) to linearize the region of quartz-like Si–O vibrations at 2200–1800 cm^{-1} ('zero-ing') (M 2015).

2.3.2. DOM

Pore water samples were lyophilized (1 μg C: 1 mg KBr) and scanned undiluted on a Digilab FTS 7000 Fourier transform spectrometer (Varian, Inc., Palo Alto, CA) with a deuterated, Peltier-cooled, triglycine sulfate detector, a KBr beam splitter, and a Pike AutoDIFF diffuse reflectance accessory (Pike Technologies, Madison, WI). Using KBr as background, duplicate spectra from separately loaded sub-samples were collected as pseudo-absorbance (log [1/Reflectance]) from 4000 to 400 cm^{-1} (4 cm^{-1} resolution) with 64 co-added scans per spectrum. Duplicate spectra were averaged. DRIFT spectra of DOM were not corrected for mineral absorbances due to low or negligible mineral contents.

2.4. DRIFT spectroscopy analysis of OM composition

Bulk SOM and DOM spectra were analyzed for specific absorbance bands representing organic functional groups that constitute OM. Absorbance bands were selected based on three criteria: (1) presence in the spectra of all samples (2) identified in previous studies on permafrost composition (Ernakovich et al., 2015; Matamala et al., 2017), and (3) local maxima (peak, shoulder). Selected bands represent diverse organic functional groups previously identified for these (Ernakovich et al., 2015) and other permafrost (Matamala et al., 2017) and peat soils (Artz et al., 2008). Band assignments (Table 1) were based on previous DRIFT and NMR studies of DOM derived from soil and plant biomass and similar functional groups were measured for DOM and bulk SOM. Band absorbance intensities were calculated relative to a linear tangential baseline with zero points at local absorbance minima.

2.5. Potential soil extracellular enzyme activities

The potential activities of six hydrolytic enzymes involved in C-, N-, and P-depolymerization were determined as described by Ernakovich et al. (2017): β-glucosidase (Enzyme Commission 3.2.1.21), cellobiohydrolase (EC 3.2.1.91), xylosidase (EC 3.2.1.37), N-acetylglucosaminidase (EC 3.2.1.50), leucine aminopeptidase (EC 3.4.1.1), and acid phosphomonoesterase (EC 3.1.3.2). Soil enzyme activities were assayed at the end of the incubation at both 1 and 15 °C using fluorescently-labeled substrates (4-methylumbelliferyl [MUB] or 4-methylcoumarin [MUC]) in 96-deep well plates (Bell et al., 2013). Briefly, 1 g of soil was homogenized in 91 mL of 0.05 mol L^{-1} sodium acetate buffer (pH 6.5) in a Waring blender. While slurries mixed on a stir plate (45 s), 800 μL soil slurry and 200 μL of 200 μmol L^{-1} fluorescing substrates were pipette-transferred to the sample assay wells, for a final substrate concentration of 40.0 nmol L^{-1}. Previous work on Arctic soils indicates this substate concentration saturates the hydrolytic enzymes (Koyama et al., 2013). Thus, measured activities approximate V_{max}, averting false negatives when comparing enzyme activities (Deng et al., 2017; Margenot et al., 2018). Substrate-free controls were also prepared. Plates were incubated at 15 °C for 6 h or 1 °C for 24 h. Reactions were terminated by adding 5 μL of 0.5 mol L^{-1} NaOH to each sample; a clear supernatant was obtained by plate centrifugation (350×*g*, 3 min). Fluorimetry was conducted using 250 μL of assay supernatant in black 96-well plates at an excitation wavelength of 365 nm and an emission wavelength of 450 nm. Soil enzyme activities were calculated as nmol substrate g^{-1} soil h^{-1}. Enzyme activity ratios were calculated for C:N, C:P, and N:P enzymes to identify potential changes in enzymatic stoichiometry of C, N and P mineralization (Koyama et al., 2013). Q_{10} values (i.e., the ratio of enzyme activities at 1 and 15 °C) were used to estimate relative temperature responses across C, N, and P-acquiring enzymes.

2.6. Statistical analyses

Differences in the relative absorbance of organic functional groups by depth, temperature, and redox (including all three-way interactions) were tested using Tukey's test (α = 0.05) with Proc GLM in SAS v9.4

Table 1
Assignments used to interpret absorbance bands in DRIFT spectra of soils and thaw DOM from 0 to 10 cm and 16–25 cm layers of permafrost.

SOM	DOM	
Wn (cm^{-1})	Wn (cm^{-1})	Assignment
3400	3334	hydroxyl O–H, amine N–H
2923	–	aliphatic C–H stretch
2853	–	Carbonates and/or aliphatic C–H stretch
1652	1656	aromatic C═C and/or amide C═O and ketone C═O
1558	1540	aromatic C═C and/or amide C═O
1456	–	carboxyl and/or ester C–O and aliphatic C–H bend
1420	1416 & 1384	N–H and C–N and/or aliphatic C–H bend
1252	–	amide N–H, carboxylate and/or phenol C–O
–	1201	amide N–H, carboxylate and/or phenol C–O, ester C–O
1111	1124	ester C–O
–	1095	ester C–O
1020	1042	polysaccharide ester C–O

Peak absorbance intensities were calculated relative to a linear tangential baseline with zero points at local absorbance minima for SOM at 3680, 3018, 2770, 1795, 1605, 1487, 1362, 1362, 1339, and 813 cm^{-1}, and for DOM at 3771, 3015, 834, 1282, and 943 cm^{-1}.

(SAS Institute, Cary, NC). The F-statistic was calculated to compare the relative magnitude of depth, redox, and temperature on the absorbance of SOM and DOM bands measured by DRIFT spectroscopy. Relative absorbance values were first tested for normality of residuals using the Shapiro-Wilk's test and for homoscedasticity using Levene's test. The relative absorbance of two SOM bands (2853 cm^{-1} at 0–10 cm depth and 1456 cm^{-1} at both depths) were power transformed to satisfy normality of residuals and log-transformed to meet homoscedasticity, respectively. To satisfy normality of the residuals, values of DOM bands 1656, 1540, 1384 cm^{-1} at 0–10 cm depth were log transformed, and 1095 cm^{-1} at 16–25 cm depth was power transformed. DOM bands at 1416 cm^{-1} at 0–10 cm depth and 1540 cm^{-1} at 16–25 cm depth were log-transformed for homoscedasticity.

We simultaneously visualized relationships between SOM and DOM composition, the potential activities of six hydrolytic enzymes, and pH—a master variable controlling nutrient availability and chemical reactions—using constrained analysis of principal components (cap-scale) (Oksanen et al., 2007). Bray-Curtis dissimilarities were computed from *z*-transformed band intensities and environmental drivers, with p-values calculated over 999 permutations (Fig. 4, $p = 0.01$).

Relationships between the dependent variable of interest (SOM or DOM band) and potential explanatory variables were formally evaluated using multiple linear regression models. Highly correlated variables (SI Fig. 1) were identified using variation inflation factors (VIF) calculated for each parameter in the model using the *vif* function in the R *car* package (Fox and Monette, 1992; R Core Team, 2018). Those with a VIF score >2 were sequentially removed until only independent variables remained (Duffy et al., 2016; Zuur et al., 2009, 2010). Temperature, redox, pH, and the hydrolytic activities of BG, LAP, and NAG were ultimately retained. Mixed effects regression models were tested first, including the permafrost core each sample was taken from as a random effect. The random effect was significant for three SOM bands (1652, 1456, and 1020 cm^{-1}) and one DOM band (1416 cm^{-1}). For the remaining bands, stepwise linear regressions were conducted using the *step* function in the R *stats* package (Lynch et al., 2019b). One DOM band was normalized using a boxcox power transformation in the R *MASS* package (SOM 1252 cm^{-1}) and one was log-transformed (DOM 1416 $^{-1}$) to meet the assumptions of normality.

3. Results

3.1. SOM bands

SOM bond absorbances were relatively unaffected by experimental thaw conditions (redox, temperature, SI Fig. 2), but differed strongly by permafrost depth (Fig. 1, SI Table 1). SOM from the deeper permafrost horizon (16–25 cm) displayed a higher relative absorbance of polysaccharide ester C–O (1111 cm^{-1}, 1020 cm^{-1}) and phenol C–O (1252 cm^{-1}) bonds than shallow permafrost (0–10 cm). In contrast, shallow permafrost displayed a greater relative absorbance of bands corresponding to aliphatic C–H stretch (2923 cm^{-1}) and bend (1456, 1420 cm^{-1}), alcohol O–H (3400 cm^{-1}) and/or amide N–H (3400 cm^{-1}, 1420 cm^{-1}), and amide C═O (1656 cm^{-1}) functional groups. The relative absorbance of bands corresponding to aliphatic C–H (2583 cm^{-1}) and amide C═N and N–H (1558 cm^{-1}) did not differ by depth.

3.2. DOM bands

Thaw condition (redox, temperature) strongly influenced DOM functional group composition, with no significant main effect of permafrost depth (Table 2), in contrast to variability in SOM bands during thaw. Significant three-way interactions between permafrost depth, redox, and temperature explained the relative abundance of alcohol O–H and amine N–H bands (3334 cm^{-1}), aromatic C═C and amide and/or ketone C═O bands (1656 cm^{-1}) (Fig. 2). Alcohol and amine bands were less abundant after 90 days at 15 °C than 1 °C in shallow drained and deep saturated horizons, conditions that most likely reflect in situ thaw. Surface permafrost samples thawed at 15 °C displayed lower relative absorbance of aromatic and C═O bonds under drained conditions, but greater abundance under saturated conditions. Similarly, amide and/or ketone C═O bands (1540 cm^{-1}) were enriched under warm, saturated conditions in deep permafrost horizons. The relative abundance of polysaccharide ester C–O bonds (1124 cm^{-1}, 1095 cm^{-1}, 1042 cm^{-1}) were influenced by both temperature and redox. At 15 °C, both 1124 cm^{-1} (0–10 cm deep) and 1095 cm^{-1} (16–25 cm deep) were significantly more abundant in drained than saturated conditions; when freely drained, the relative absorbance of 1042 cm^{-1} was greater at 1 °C than 15 °C. Only three absorbance bands did not exhibit significant two- or three-way interactions (1416 cm^{-1}, 1384 cm^{-1}, 1095 cm^{-1}). Aliphatic or N–H and C–N bearing functional groups at 1416 cm^{-1} were more abundant under saturated than drained conditions, and those absorbing at 1384 cm^{-1} were more abundant at 15 °C than 1 °C. Ester C–O absorbing bands at 1095 cm^{-1} were more abundant under drained than saturated conditions.

3.3. Enzyme activities

To evaluate how extracellular enzyme dynamics modulated SOM and DOM chemistries, we conducted enzyme assays at two temperatures (15 °C and 1 °C to match incubation temperatures) to determine potential depolymerization rates relevant to in situ process rates (Fenner et al., 2005). We performed the assays in upper permafrost horizons (0–10 cm), which are more vulnerable to climate-driven thaw and cryoturbation than deeper horizons. We observed that the activities of six

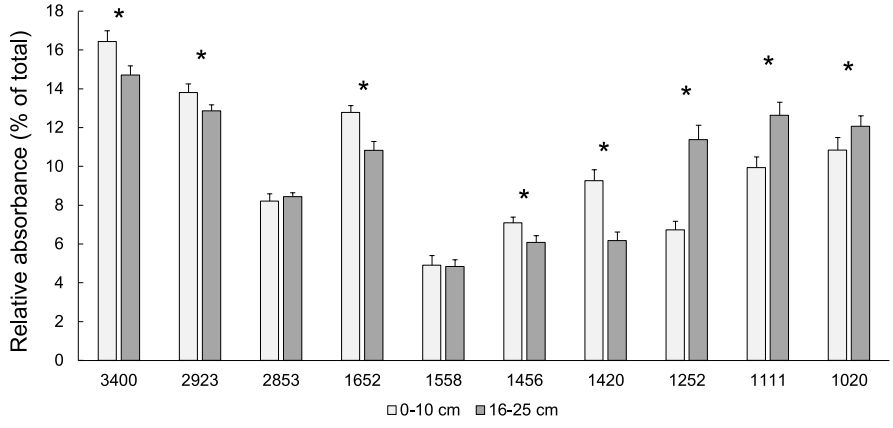

Fig. 1. Differences in the relative absorbance of organic functional groups between the 0–10 cm and 16–25 cm depth layers of permafrost (i.e., bulk SOM). Permafrost layers were subjected to simulated thaw for 90 days under varying temperature (1 °C or 15 °C) and redox (saturated or drained) conditions. Absorbance bands were detected by diffuse reflectance infrared Fourier transform (DRIFT) spectroscopy. Asterisks depict statistical differences between permafrost layers at $p < 0.05$ using a Tukey-Kramer multiple testing comparison. The relative intensity of SOM bands was not significantly influenced by redox or temperature.

Table 2
Analysis of variance (ANOVA) of absorbance intensity at 10 wavenumbers representing distinct functional groups of DOM derived from permafrost. Permafrost samples from two depths (0–10 cm, 16–25 cm) were incubated at 1 °C or 15 °C (Temperature) for 90 days under saturated or drained (Redox) thaw conditions.

FTIR Band (cm^{-1})	Depth		Redox		Temp		Depth x Redox		Depth x Temp		Redox x Temp		Depth x Redox x Temp	
	F	p	F	p	F	p	F	p	F	p	F	p	F	p
3334	1.0	0.33	0.5	0.49	**15.4**	**<0.001**	0.2	0.63	3.6	0.07	0.1	0.74	**5.0**	**0.03**
1656	1.1	0.31	**11.6**	**<0.01**	0.3	0.58	**10.6**	**<0.01**	**6.0**	**0.02**	**9.9**	**<0.001**	**8.9**	**0.01**
1540	2.3	0.14	**20.7**	**< 0.0001**	0.2	0.66	0.0	0.92	0.5	0.47	**5.4**	**0.03**	0.2	0.68
1416	2.6	0.11	**23.2**	**< 0.0001**	0.7	0.42	0.0	0.84	0.0	0.79	0.0	0.99	0.4	0.52
1384	1.0	0.31	1.2	0.28	**6.4**	**0.02**	0.6	0.45	0.1	0.74	0.1	0.82	0.5	0.49
1201	0.0	0.94	**9.2**	**<0.01**	**9.3**	**<0.01**	**4.5**	**0.04**	0.5	0.50	**9.4**	**<0.001**	0.9	0.35
1124	0.8	0.38	**21.8**	**< 0.0001**	0.0	0.98	1.0	0.32	1.0	0.32	**5.5**	**0.02**	1.5	0.23
1095	1.7	0.21	**21.6**	**< 0.0001**	0.5	0.49	0.1	0.78	0.6	0.46	1.7	0.20	0.1	0.81
1042	3.1	0.09	2.1	1.56	**35.3**	**< 0.001**	**4.8**	**0.04**	0.3	0.57	**7.4**	**0.01**	1.6	0.22

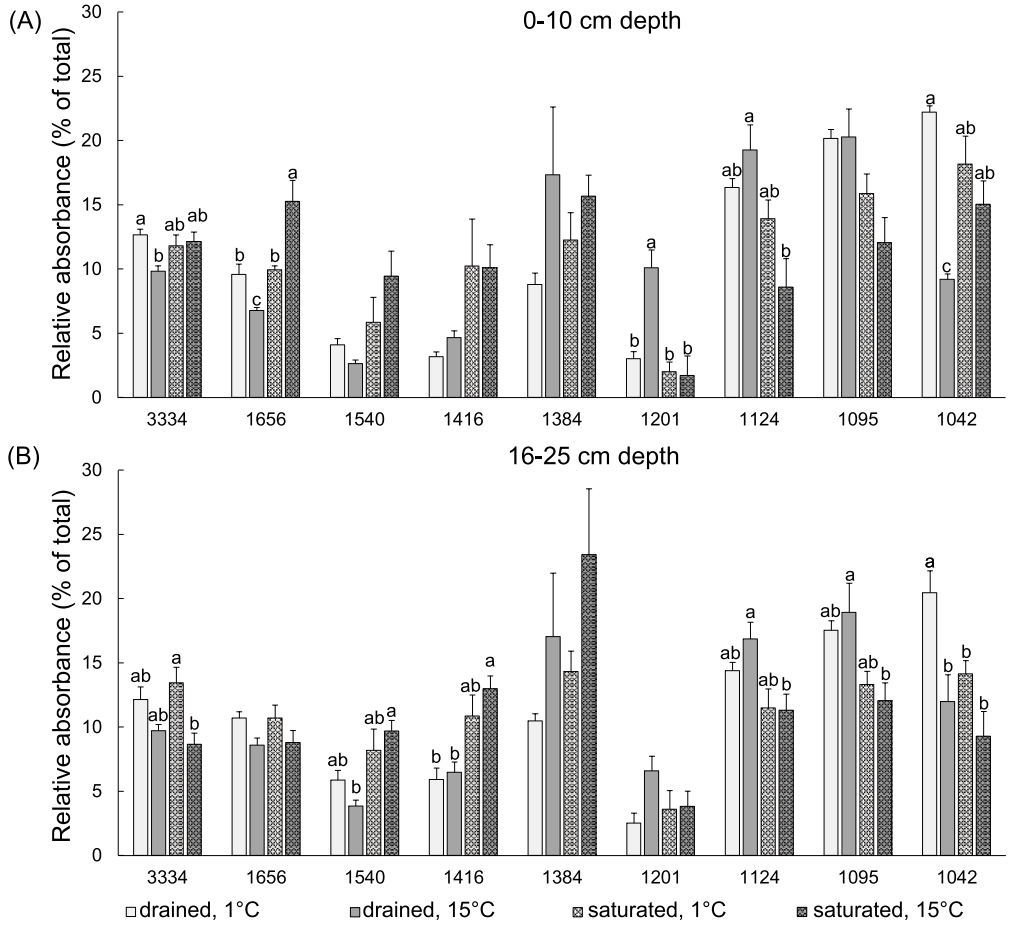

Fig. 2. Relative absorbance of organic functional groups in DOM detected by diffuse reflectance infrared Fourier transform (DRIFT) spectroscopy. Different letters indicate statistical differences among thaw treatments (redox, temperature) at $p < 0.05$ using a Tukey-Kramer multiple testing comparison.

C-, N-, and P-cycling hydrolytic soil enzymes were more directly influenced more by temperature than redox (Fig. 3). The activities of all measured enzymes were at least two-fold greater when incubated (and assayed) at 15 °C than 1 °C. Within each of the redox treatments, activities were greatest for PHOS and NAG, followed by the three C-cycling enzymes (BG, CB, XYL), and finally by LAP. The ratio of C- to N-acquiring enzymes was significantly higher in saturated than drained environments, suggesting energetic constraints will limit OM decomposition waterlogged sites while nutrient availability will limit OM decomposition within freely drained sites (SI Fig. 3). Q_{10} values were not statistically different across measured enzyme activities, except for LAP, which displayed significantly higher Q_{10} values in drained treatments incubated at 1 °C than 15 °C (5.07 ± 1.88 versus 3.51 ± 1.34, respectively; $F_{1,6} = 8.98$, $p = 0.02$).

3.4. Relationships of SOM and DOM bands with environmental variables

Consistent with results from ANOVA models, temperature and redox did not explain variance in the relative abundance of SOM functional groups. Instead, variability in six out of ten SOM band absorbances was related to the activity of C-cycling enzymes (here represented by BG). The relative absorbance of N-bearing or aliphatic functional groups (1420 cm^{-1}) was predicted by soil pH and the activities of BG and NAG. NAG, which depolymerizes chitin, also predicted shifts in the relative absorbance of aliphatic C and ester C–O bonds (1456 cm^{-1}, 1111 cm^{-1}). The activity of LAP, which hydrolyzes polypeptide bonds (Greenfield

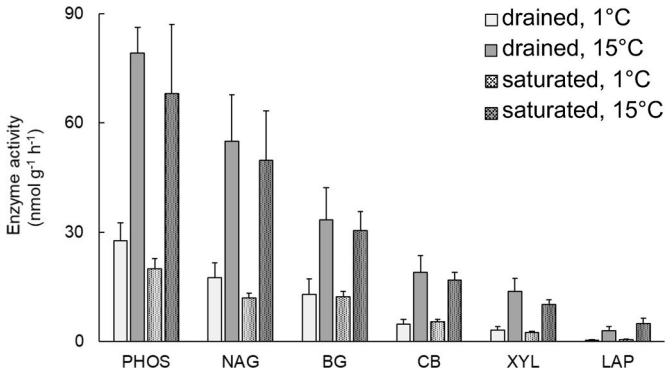

Fig. 3. Potential extracellular activities of six hydrolytic enzymes in surface permafrost layers after 90 days of simulated thaw under varying redox and temperature conditions. Enzymes are acid phosphomonoesterase (PHOS), N-acetylglucosaminidase (NAG), β-glucosidase (BG), cellobiohydrolase (CB), xylosidase (XYL), and leucine-aminopeptidase (LAP).

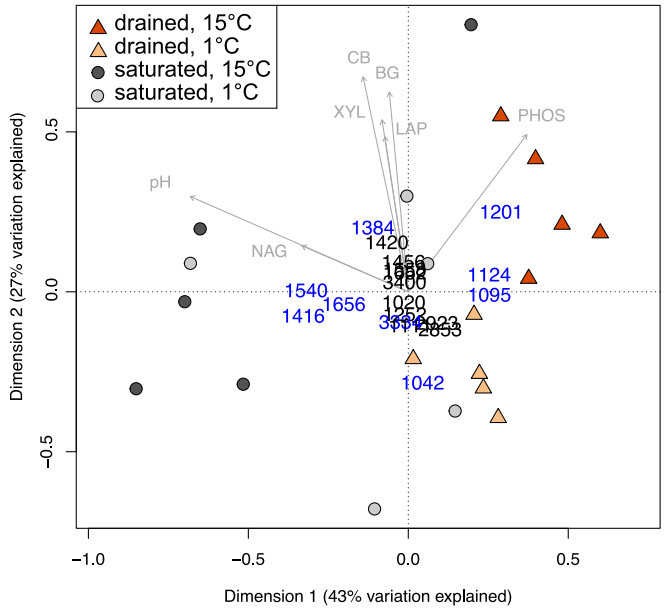

Fig. 4. Constrained analysis of principal coordinate ordination, based on Bray-Curtis dissimilarity, tests for an association between permafrost chemistry (wavenumbers are blue for DOM bands and black for SOM bands) and potential environmental drivers (gray vectors). Permafrost samples were collected from 0 to 10 cm below the maximum active layer thaw depth and incubated for 90 days at 1 °C (light shading) or 15 °C (dark shading) under saturated (gray circle) or drained (rust triangle) conditions.

et al., 2021), was related to variability in the relative abundance of C–O ester and aliphatic C–H functional groups (1456 cm^{-1}). Variability in the relative absorbance of aliphatic C bonds was influenced by pH (2923 cm^{-1}, 2853 cm^{-1}, 1020 cm^{-1}). Variance in aromatic carbon and amide C═O bonds (1558 cm^{-1}) was not influenced by temperature or redox.

In contrast, the relative absorbance of seven out of nine DOM bands was predicted by redox. Variability in only two bands was related to extracellular enzyme activities: BG was strongly related to the relative absorbance of polysaccharide CH_2, protein CH_2, C–H, or C–O bands (1384 cm^{-1}) and LAP was marginally related to alcohol O–H or amine N–H bonds (3334 cm^{-1}). We further visualized relationships between extracellular enzyme activities and shallow permafrost OM band intensities using constrained analysis of principal coordinates, a multivariate ordination method that tested for an association between permafrost chemical composition and potential environmental drivers (Oksanen et al., 2007) (Fig. 4).

The chemical composition of thawed permafrost was not only influenced by incubation conditions (redox, temperature) but also by environmental drivers (pH and potential hydrolytic enzyme activities) (Fig. 4). Within ordination space, principal coordinate 1 (Dimension 1) explained 43% of the variation across the dataset, and principal coordinate 2 (Dimension 2) explained an additional 27%. The functional chemistries of permafrost SOM were tightly clustered and less sensitive to soil redox and temperature than DOM composition, which shifted significantly as a function of incubation condition. Formal regression analyses support these dynamics; redox was retained in the best-fit model for all tested DOM bands (excepting bands 3334 cm^{-1} and 1384 cm^{-1}) but was not retained in any model predicting the relative absorbance of SOM bands (Table 3).

Permafrost samples incubated at 15 °C under drained conditions were strongly clustered and associated with the activity of alkaline phosphatase, and to a lesser extent by the activities of two C-hydrolytic enzymes that catalyze cellulose degradation, BG and CB. Drained permafrost samples were also enriched in the relative absorbance of bands corresponding to polysaccharide ester C–O or aliphatic C–H bends and/or proteinaceous compounds (DOM bands 1095 cm^{-1}, 1124 cm^{-1}, 1201 cm^{-1}, 1384 cm^{-1}, and SOM band 1420 cm^{-1}), matching ANOVA results (Table 2).

The chemical composition of permafrost samples incubated under saturated conditions were highly variable, particularly those thawed at 15 °C. Overall, permafrost thawed under saturated conditions were primarily associated with the activity of NAG and pH. saturated samples were marginally less acidic than drained samples (pH = 6.35 ± 0.16 vs. 5.97 ± 0.15, p = 0.09) and relatively enriched in aromatic C═C or amide C═O bearing compounds (DOM bands 1540 cm^{-1} and 1656 cm^{-1}), polysaccharide ester C–O bonds (DOM band 1042 cm^{-1}), and aliphatic groups (DOM band 1416 cm^{-1}). Samples thawed at 1 °C were also highly variable, but many clustered near the origin along with SOM bands.

4. Discussion

Permafrost thaw liberates organic matter previously sequestered in frozen soils into active biogeochemical cycles (Tank et al., 2020). Numerous studies have shown permafrost-derived organic matter is vulnerable to microbial decomposition (Abbott and Jones, 2015; Gillespie et al., 2014; Mackelprang et al., 2011; Schuur et al., 2009; Ward and Cory, 2015) and that the mobilization and lateral transport of particulate and dissolved organic matter (DOM) can lead to significant soil C losses (Plaza et al., 2019). The pulse of OM and nutrients from permafrost degradation may transform the ecological functioning of aquatic ecosystems (Bruhn et al., 2021) and impact the Arctic C balance. However, it remains unclear how permafrost depth, thaw temperature, and prevailing redox conditions modulate enzymatic catalysis of insoluble versus soluble OM pools.

Using a 90-day simulated thaw experiment, we found that permafrost depth and potential extracellular enzyme activities significantly influenced soil organic matter (SOM) chemistry, while redox and pH drove shifts in soluble OM pools. We also demonstrated the utility of spectral subtractions for improving the sensitivity of DRIFT spectroscopy to organic functional groups in soil samples. This approach may be particularly useful for investigating subtle changes in OM chemistry induced by realistic thaw conditions (Calderón et al., 2013), and for identifying DRIFT spectroscopy-detectable OM moieties that serve as early indicators of SOM decomposition. We suggest depth-resolved analyses of permafrost vulnerability to enzymatic hydrolysis can help explain different patterns in SOM versus DOM cycling that may help constrain modeled projections of Arctic C storage during global change.

Table 3
Results of stepwise multiple linear regression (MLR) models displaying the influence of potential explanatory variables on the relative absorbance of SOM or DOM functional groups (Band Wn). Surface permafrost soils (0–10 cm) were thawed for 90 days under different temperature (1C, 15C) and redox (drained, saturated) conditions. Potential explanatory variables were autoscaled and retained based on VIF and AICc criteria. Multiple regression mixed effects models were used when the random effect of permafrost core was significant; otherwise, standard MLR was applied. The level of significance is reported as * $p < 0.05$, ** $p < 0.01$, or *** $p < 0.001$. Model-retained enzymes are β-glucosidase (BG), N-acetylglucosaminidase (NAG), and leucine-aminopeptidase (LAP).

Sample type	Band Wn (cm^{-1})	Temp	Redox	pH	BG	NAG	LAP	Random Effect	Adjusted R^2
SOM	3400				*				0.17
SOM	2923			***					0.41
SOM	2853			**					0.35
SOM	1652				**			**	0.62
SOM	1558								
SOM	1456				**	**	**	**	0.74
SOM	1420			***	***	***			0.76
SOM	1252				*				0.13
SOM	1111				**	*			0.25
SOM	1020			*				**	0.53
DOM	3334						*		0.15
DOM	1656		***						0.50
DOM	1540		***	*					0.67
DOM	1416		*					*	0.36
DOM	1384			*	***				0.58
DOM	1201	***	**						0.55
DOM	1124		**						0.34
DOM	1095		**	*					0.50
DOM	1042	***	**	**					0.70

4.1. Permafrost SOM composition determined by thaw depth

Neither temperature nor redox were significant predictors of SOM functional group composition during simulated thaw. Instead, SOM chemistry differed strongly by depth. Deeper permafrost horizons (16–25 cm) had a higher relative abundance of SOM functional groups related to phenols (1252) and polysaccharides (1020–1120) than shallow permafrost (0–10 cm), which could reflect the build-up of fermentation byproducts (Lynch et al., 2019) or selective retention of plant-derived lignin phenols on iron oxides (Wang et al., 2017). SOM pools in upper permafrost horizons (0–10 cm) were enriched in a variety of functional groups, including markers for fatty acids and their degradation byproducts (C–H bonds of aliphatics and C═O bonds of ketones), proteins, and alcohol and amine functional groups. The presence of readily decomposable compounds at the active layer-permafrost interface may increase microbial substrate availability as shallow permafrost horizons thaw and mix via cryoturbation (Ernakovich et al., 2015; Joss et al., 2022). However, we previously found that 90 days of simulated thaw mineralized less than 1% of initial SOC stocks, with only 0.32% mineralized in drained and 0.18% in saturated treatments thawed at 1 °C, and 0.90% in drained and 0.61% in saturated treatments thawed at 15 °C (Ernakovich et al., 2017), suggesting the molecular composition of recently liberated OM will exert an important control on microbial metabolism and substrate mineralization (Ward and Cory, 2015). Multivariate ordination and regression analyses revealed strong clustering of SOM functional groups and relative insensitivity to environmental drivers such as temperature and redox. Instead, variability in SOC functional group composition was driven the potential activities of two hydrolytic enzymes (BG and NAG) and solution pH, suggesting microbial activity (and indirectly, soil chemistry) exerts a critical control on initial stages of SOM decomposition (Koyama et al., 2013). Although not directly measured here, rates of SOC decomposition will be modulated by N-availability. Currently, up to 90% of N in yedoma systems is locked in permafrost (Strauss et al., 2022). Liberating this key resource could stimulate active layer productivity in terrestrial and aquatic environments and alleviate constraints on microbial decomposition (Frey and McClelland, 2009; Koyama et al., 2013; Schimel et al., 2004). Under nominal experimental field warming (+1 °C), pools and fluxes of organic N were an order of magnitude higher than inorganic N, which can reflect seasonal trends in microbial biomass (i.e., growth and death) (T. Weedon et al., 2012) and highlights the role hydrolytic enzymes will play during permafrost thaw.

4.2. DOM composition driven by redox status

The functional composition of DOM liberated from thawing permafrost was highly variable and strongly influenced by redox status. Although the chemical composition of DOM was similar across depth, DOM released from deeper permafrost horizons thawed under saturated conditions at 15 °C were enriched in ketones and reduced in alcohol and amine functional groups relative to other treatments. Within shallow permafrost horizons, variability in DOM functional group composition was driven by redox status; drained treatments were relatively enriched in polysaccharide (1 °C) and phenolic, ester, and carboxylate (15 °C) functional groups. We previously observed rapid polysaccharide depletion from active layer and permafrost soils collected at the same site, particularly when incubated under warm, drained conditions (Ernakovich et al., 2017). Polysaccharides may subsidize metabolism under conditions that would otherwise limit decomposition rates, such as low temperature, nutrient, and oxygen availability (Melle et al., 2015; Nadelhoffer et al., 1991; Wild et al., 2016). We also found that carboxylates accumulated over the course of decomposition and with depth (Ernakovich et al., 2017) consistent with previous evaluations of permafrost (Ernakovich et al., 2015; Haberhauer et al., 1998). Rapid shifts in microbial community structure following thaw (Coolen et al., 2011; Hultman et al., 2015; Mackelprang et al., 2011) may induce corresponding shifts in the metabolic pathways expressed at the community level (Doherty et al., 2020; Monteux et al., 2020), particularly as stress-dominated metabolism is replaced by degradation of diverse substrates (Coolen and Orsi, 2015; Frank-Fahle et al., 2014; Hultman et al., 2015). This transition is predicted to upregulate the expression of core carbohydrate metabolism, including cellobiose and sugar transport systems (Mackelprang et al., 2011). The functional chemistries of DOM thawed in saturated conditions at 1 °C clustered near SOM bands, suggesting less extensive microbial transformation and processing. These results emphasize the importance of landscape position in cycling thawed organic matter. For example, cold, waterlogged sites may continue accumulating OM due to constraints on microbial metabolism. In contrast, OM released from warmer, drained sites (i.e., hillslopes or shallow permafrost) may be more extensively processed in-situ.

DOM functional group composition was highly variable in saturated treatments but showed a relative accumulation of ketones and aromatic

compounds. Ketones are a prevalent decomposition byproduct of fatty acid metabolism and have been previously used as biomarkers for recycled microbial biomass (Baumann et al., 2021). Several Archaea in boreal saturated peatlands were found to degrade fatty acids and acquire energy through anaerobic respiration, using organic acids such as fumarate and organosulfonate as terminal electron acceptors (Lin et al., 2015). Similarly, permafrost bacterial communities have been found to preferentially degrade aromatic and oxidized lignins during initial stages of permafrost decomposition (Zhou et al., 2020). Zhou et al. (2020) found that the depletion of aromatic compounds, which are not very IR active, during thaw progression was coupled with declining metabolic and taxonomic diversity, ultimately reducing the production of microbial-derived lipids and proteins. We previously observed relatively high N_2O production from permafrost incubated under drained conditions and redox potentials within the denitrification range (Seo and DeLaune, 2010), suggesting anaerobic metabolism could be widespread, particularly within soil microsites (Brune et al., 2000). Although microbial diversity is typically reduced in anoxic systems, the use of diverse terminal electron acceptors across the redox ladder and *ex vivo* OM modification through enzymatic catalysis may increase molecular heterogeneity within the DOM pool (Liang et al., 2017). The net effect of DOM heterogeneity on the efficiency of microbial metabolism remains unclear, but greater resource availability, as observed in upper permafrost horizons (Ernakovich and Wallenstein, 2015), may drive DOM assimilation and biomass synthesis. Encountering compounds with a high relative abundance could select for taxa with compatible enzymatic scaffolds and metabolic pathways (Zuppinger-Dingley et al., 2014), driving niche differentiation and increasingly efficient substrate use (Hess et al., 2021; Nuccio et al., 2020; Sokol and Bradford, 2019).

4.3. Effect of hydrolytic enzyme activities on permafrost chemistry

Extracellular enzyme activities offer a powerful tool to investigate feedbacks between permafrost thaw and SOM chemistry because microbial physiology and enzyme activities are directly affected by temperature (Allison et al., 2010; Wallenstein et al., 2010). However, linking potential extracellular enzyme activities to shifts in C cycling must be interpreted cautiously. First, a substantial amount of catalytic activity—up to 75% in some instances (Knight and Dick, 2004)—may be derived from enzymes stabilized in the soil matrix that are no longer associated with viable cells (Nannipieri et al., 2018). Coined the 'abiontic pathway' in the 1960s (McLaren et al., 1957; Skujins, 1967), this phenomenon may be particularly influential in permafrost systems where enzymes can adsorb on recently exposed inorganic surfaces (clays, irons oxides, and hydroxides) or complex with organic colloids in C-rich deposits. Second, mineralization processes often involve sequential catalysis of polymeric compounds by multiple enzymes. These biochemical transformations are not fully captured when measuring the potential activities of single enzymes (an exception being CB and BG, which sequentially catalyze cellulose degradation). Finally, encoding and secreting extracellular enzymes is energetically costly (Schimel and Weintraub, 2003). Substantial investment in enzyme production is only worthwhile if substrate availability is sufficiently high, increasing the chance that enzyme-secreting microorganisms assimilate depolymerized products (Allison, 2005). As a result, even smaller, energetically favorable compounds (carbohydrates, amino sugars) may persist if (1) substrates are present at low concentrations, (2) compatible metabolic pathways are not expressed within the microbial community, or (3) substrates, or the enzymes themselves, are adsorbed to mineral surfaces (Swenson et al., 2015). Despite these caveats, perennially frozen soils are enriched in relatively large molecular-weight plant-derived oligosaccharides (Mackelprang et al., 2017; Taş et al., 2018) that must be converted into assimilable monomers prior to microbial uptake (Emerson et al., 2018). The primary way to achieve this is via extracellular hydrolysis. As a result, changes in enzyme catalytic capacity (V_{max}) can reveal underlying shifts in microbial function. For example, seasonal shifts in nutrient availability may alter short-term catalytic efficiency (Melle et al., 2015; Tian et al., 2020; Wallenstein et al., 2009) while climate-driven changes in plant inputs and soil properties are predicted to control longer-term shifts in enzyme kinetics (V_{max}, K_m) and Arctic-carbon trajectories (Allison et al., 2010; Sistla and Schimel, 2013). Our results suggest pairing DRIFT spectroscopy with potential extracellular enzyme assays can identify C functional groups that serve as sensitive indicators of permafrost decomposition.

Potential enzyme activities were highly temperature sensitive (Pearson correlations range from 0.6 to 0.8; Q_{10} values range from 3.51 to 11.79, with LAP exhibiting the highest Q_{10} variability), which is consistent with warming accelerating microbial activity and the Q_{10} sensitivity of extracellular enzymes (Wallenstein et al., 2009). Although univariate and multivariate analyses suggest redox conditions exerted a greater direct influence on DOM composition than temperature alone, these ecosystem factors are inextricably linked (Lynch et al., 2019a; Tank et al., 2018). For example, warming will increase permafrost thaw (Smith et al., 2022), stimulate microbial growth (Coolen and Orsi, 2015), and accelerate rates of enzyme catalysis (Davidson and Janssens, 2006). These processes could drive down redox gradients directly, by inundating soil micropores, or indirectly, by accelerating the activity of aerobic communities that exhaust terminal electron acceptors higher on the redox ladder and opening niches for anaerobic communities.

The dynamic relationship between SOM functional group chemistry and the potential activities of extracellular enzymes suggests the hydrolysis of insoluble OM is a rate-limiting step in permafrost soils. Within the upper permafrost horizon, the activities of two hydrolytic enzymes, β-glucosidase (BG) and chitinase (NAG), were strongly correlated with variability in SOM chemistry (Table 3). BG—which cleaves the alternate glycosidic bonds of cellulose to form cellobiose (Shrotri et al., 2017)—explained variability in six SOM functional groups corresponding to polysaccharide, protein, C–H, and C–O functional groups. Our results suggest there is a direct link between the relative abundance of C functional groups in SOC pools and the potential activities of enzymes acting on those substrates (Margenot et al., 2017b). However, underlying differences in permafrost chemistry will govern microbial community composition, modulating rates of enzyme production (and thus assayed activities) and substrate depolymerization. As a result, observed relationships between SOM chemistry and enzyme activity better describe linkages, rather than causal relationships. For example, the association of BG with aliphatic functional groups may result from the indirect release of C–H, as aliphatic groups are to some extent unavoidably part of the same or co-occurring compounds as C–O, or the association of glucose-containing compounds with fatty acids. Indeed, the catabolic breakdown of carbohydrate polymers, particularly of plant cell wall components (i.e., cellulose, hemicellulose, lignin), is a fundamentally synergistic process as enzymes targeting individual carbohydrate complexes will influence the availability and turnover of all others (Levasseur et al., 2013). Similarly, NAG was a significant predictor of variability in carboxyl, ester, aliphatic, and N-bearing functional groups (i.e., N–H and C–N bends). Chitinase hydrolyzes glucosidic bonds to release smaller, N-containing organic compounds that can be mineralized to inorganic N (Gooday, 1994; Olander and Vitousek, 2000).

The most biologically active systems (surface permafrost horizons incubated at 15 °C under drained conditions) were strongly associated with potential acid phosphomonoesterase (AP) activity. In turn, AP activity was strongly correlated with three DOM bands corresponding to ester C–O functional groups. Because phosphatase enzymes have wide substrate affinities (Sinsabaugh et al., 1993), their synthesis may alleviate energy constraints on microbial metabolism (Spohn and Kuzyakov, 2013; Steenbergh et al., 2011; Wang et al., 2016), representing an overlooked driver of C cycling in permafrost soils. We previously observed that microbial biomass P and resin-extractable orthophosphate-P concentrations were similar (and low) across thaw conditions (Ernakovich et al., 2017), but here we found that AP activity increased

by nearly a factor of six when permafrost was thawed at 15 °C relative to 1 °C. In addition to temperature-driven increases in AP activity, abiotic pathways could play an equally important regulatory role in P and C cycling. AP complexation on clays and/or poorly crystalline Fe and Al oxhydroxides (Kleber et al., 2021; Vogel et al., 2014) could attenuate C mineralization in Arctic soils. The reductive dissolution of Fe–P complexes under anoxic conditions attenuates AP activity by reducing geochemical competition for mineralized P (Steenbergh et al., 2011). Supporting this line of reasoning, we found that N/P-cycling ratios were elevated in more drained (N:P ~0.38 at ~360 mV, n = 8) than saturated (N:P ~1 at ~250 mV, n = 14) systems, suggesting extracellular enzyme investment is co-governed through biotic and abiotic processes.

In contrast, permafrost samples thawed under saturated conditions clustered with solution pH and NAG activity and were enriched in three functional groups related to proteinaceous compounds (aromatic C═C, amide C═O, and ketone C═O bands). While NAG catalyzes chitin depolymerization, mineralization of N-bearing compounds can often be coupled with energy acquisition (Farrell et al., 2014; Mori et al., 2021). Typically, NAG activity declines as soil pH increases (Fujita et al., 2018; Sinsabaugh et al., 2016), with a pH optimum between 4 and 6 (Zeglin et al., 2007), as observed in our soils, where samples thawed under saturated conditions were slightly less acidic and had higher NAG activities than those thawed under drained conditions. We also observed lower C/N-cycling ratios in drained than saturated environments. These results suggest microbial communities in drained environments will become progressively nutrient limited while those in anoxic microsites may experience greater energy limitation. Predicted increases in primary productivity and nutrient availability may offset these trends, particularly as deciduous shrubs and associated arbuscular mycorrhizae expand across high-latitude systems (McLaren et al., 2017; Sturm et al., 2001, 2005).

4.4. Scaling from laboratory incubations to ecosystem-relevance

Deeper permafrost layers have a greater abundance of unsaturated mineral phases that may sorb OM and reduce substrate availability for microbial metabolism. If microbial communities are less diverse and abundant than surface communities and must also contend with greater substrate adsorption, there is a lower likelihood of successful decomposer-substrate interaction (Schnecker et al., 2015). The decoupling of SOM properties and microbial community composition could thus disincentive the production of extracellular enzymes and impair the metabolic ability of the microbial community to utilize deep permafrost-derived organic matter (Schnecker et al., 2014). However, cyroturbation is also predicted to increase with climate warming (Herndon et al., 2020), translocating particulate and dissolved OM from active layer to upper permafrost horizons (Bockheim and Tarnocai, 1998). These processes currently account for up to 20% of subsoil C storage (Gentsch et al., 2015; Gundelwein et al., 2007). Results from an Arctic thermokarst chronosequence showed that iron-associated C more than doubled within the first 50 years of soil development (Joss et al., 2022). Effects on C mineralization rates remain unclear as iron-C interactions can inhibit OC mineralization by adsorbing substrates and stabilizing soil aggregates (Gentsch et al., 2018; Hemingway et al., 2019; Joss et al., 2022) while iron oxides could enhance decomposition in anoxic soils by serving as terminal electron acceptors (Herndon et al., 2017; Wang et al., 2020). Results from a mineralization experiment found that subducted, OM-rich horizons exhibited the same C mineralization potential as mineral soils within the permafrost horizon (Gillespie et al., 2014). As a result, the vulnerability of permafrost C to decomposition will be partly regulated by redox status and the flux of nutrients, enzymes, and DOM from carbon-rich active layer horizons into subsoil environments (Čapek et al., 2015; Ernakovich et al., 2017; Gentsch et al., 2015).

5. Conclusions

The balance between landscape-level C retention and loss is partially controlled by the physicochemical reactivity of DOM (Kalbitz et al., 2003; Kellerman et al., 2014), DOM-enzyme interactions, and abiotic factors, including depth-variable redox gradients (Lipson et al., 2012), residence time within the catchment (Battin et al., 2009; Mu et al., 2017; Zhang et al., 2017), and proximity of available mineral surfaces for complexation (Lehmann et al., 2008; Schmidt 2011). Landscape position will therefore play a critical role in determining how exported OC structures energy and nutrient delivery to downslope (or downstream) ecosystems and will determine whether Arctic watersheds remain a globally relevant C sink (Woods et al., 2011). Our works suggests a holistic view of feedbacks between redox status, temperature, potential extracellular enzyme activities, and the chemical composition of permafrost is appropriate.

Disclaimer

The authors declare no conflicts of interest.

Declaration of competing interest

The authors declare that they have no known competing financial interests or personal relationships that could have appeared to influence the work reported in this paper.

Data availability

Data will be made available on request.

Acknowledgements

This work was supported by awards to Jessica Ernakovich by the National Science Foundation (Graduate Research Fellowship Program and Doctoral Dissertation Improvement Grant). We would like to thank Claire Freeman for assistance with pore water extractions and Dr. Matthew Wallenstein for help designing the laboratory incubation experiment.

Appendix A. Supplementary data

Supplementary data to this article can be found online at https://doi.org/10.1016/j.soilbio.2023.108991.

References

Abbott, B.W., Jones, J.B., 2015. Permafrost collapse alters soil carbon stocks, respiration, CH4, and N2O in upland tundra. Global Change Biology 21, 4570–4587. https://doi.org/10.1111/gcb.13069.

Allison, S.D., 2005. Cheaters, diffusion and nutrients constrain decomposition by microbial enzymes in spatially structured environments. Ecology Letters 8, 626–635. https://doi.org/10.1111/j.1461-0248.2005.00756.x.

Allison, S.D., Wallenstein, M.D., Bradford, M.A., 2010. Soil-carbon response to warming dependent on microbial physiology. Nature Geoscience 3, 336–340. https://doi.org/10.1038/ngeo846.

Anderson, J.U., 1961. An improved pretreatment for mineralogical analysis of samples containing organic matter. Clays and Clay Minerals 10, 380–388.

Artz, R.R.E., Chapman, S.J., Robertson, A.H.J., Potts, J.M., Laggoun-Défarge, F., Gogo, S., Comont, L., Disnar, J.-R., Francez, A.-J., 2008. FTIR spectroscopy can be used as a screening tool for organic matter quality in regenerating cutover peatlands. Soil Biology and Biochemistry 40, 515–527.

Battin, T.J., Kaplan, L.a., Findlay, S., Hopkinson, C.S., Marti, E., Packman, A.I., Newbold, J.D., Sabater, F., 2009. Biophysical controls on organic carbon fluxes in fluvial networks. Nature Geoscience 2, 595. https://doi.org/10.1038/ngeo602, 595.

Battin, T.J., Luyssaert, S., Kaplan, L.A., Aufdenkampe, A.K., Richter, A., Tranvik, L.J., 2009. The boundless carbon cycle. Nature Geoscience 2 (9), 598–600.

Baumann, K., Eckhardt, K.-U., Acksel, A., Gros, P., Glaser, K., Gillespie, A.W., Karsten, U., Leinweber, P., 2021. Contribution of biological soil crusts to soil organic matter composition and stability in temperate forests. Soil Biology and Biochemistry 160, 108315.

Bell, C.W., Fricks, B.E., Rocca, J.D., Steinweg, J.M., McMahon, S.K., Wallenstein, M.D., 2013. High-throughput fluorometric measurement of potential soil extracellular enzyme activities. Journal of Visualized Experiments. https://doi.org/10.3791/50961.

Biskaborn, B.K., Lanckman, J.-P., Lantuit, H., Elger, K., Streletskiy, D.A., Cable, W.L., Romanovsky, V.E., 2015. The new database of the global terrestrial network for permafrost (GTN-P). Earth System Science Data 7, 245–259.

Bockheim, J.G., Tarnocai, C., 1998. Recognition of cryoturbation for classifying permafrost-affected soils. Geoderma 81, 281–293.

Borden, P.W., Ping, C.-L., McCarthy, P.J., Naidu, S., 2010. Clay mineralogy in arctic tundra Gelisols, northern Alaska. Soil Science Society of America Journal 74, 580–592.

Bruhn, A.D., Stedmon, C.A., Comte, J., Matsuoka, A., Speetjens, N.J., Tanski, G., Vonk, J. E., Sjöstedt, J., 2021. Terrestrial dissolved organic matter mobilized from eroding permafrost controls microbial community composition and growth in Arctic coastal zones. Frontiers of Earth Science 9, 640580.

Brune, A., Frenzel, P., Cypionka, H., 2000. Life at the oxic–anoxic interface: microbial activities and adaptations. FEMS Microbiology Reviews 24, 691–710.

Calderón, F., Haddix, M., Conant, R., Magrini-Bair, K., Paul, E., 2013. Diffuse-reflectance Fourier-transform mid-infrared spectroscopy as a method of characterizing changes in soil organic matter. Soil Science Society of America Journal 77, 1591–1600.

Čapek, P., Diáková, K., Dickopp, J.-E., Bárta, J., Wild, B., Schnecker, J., Alves, R.J.E., Aiglsdorfer, S., Guggenberger, G., Gentsch, N., 2015. The effect of warming on the vulnerability of subducted organic carbon in arctic soils. Soil Biology and Biochemistry 90, 19–29.

Chen, L., Liang, J., Qin, S., Liu, L.I., Fang, K., Xu, Y., Ding, J., Li, F., Luo, Y., Yang, Y., 2016. Determinants of carbon release from the active layer and permafrost deposits on the Tibetan Plateau. Nature Communications 7, 1–12.

Coolen, M.J.L., Orsi, W.D., 2015. The transcriptional response of microbial communities in thawing Alaskan permafrost soils. Frontiers in Microbiology 6, 197.

Coolen, M.J.L., van de Giessen, J., Zhu, E.Y., Wuchter, C., 2011. Bioavailability of soil organic matter and microbial community dynamics upon permafrost thaw. Environmental Microbiology 13, 2299–2314.

Davidson, E. a, Janssens, I. a, 2006. Temperature sensitivity of soil carbon decomposition and feedbacks to climate change. Nature 440, 165–173. https://doi.org/10.1038/nature04514.

Deng, S., Dick, R., Freeman, C., Kandeler, E., Weintraub, M.N., 2017. Comparison and standardization of soil enzyme assay for meaningful data interpretation. Journal of Microbiological Methods 133, 32–34.

Doherty, S.J., Barbato, R.A., Grandy, A.S., Thomas, W.K., Monteux, S., Dorrepaal, E., Johansson, M., Ernakovich, J.G., 2020. The transition from stochastic to deterministic bacterial community assembly during permafrost thaw succession. Frontiers in Microbiology 11, 596589.

Dohnalkova, A., Tfaily, M., Smith, A., Chu, R., Crump, A., Brislawn, C., Varga, T., Shi, Z., Thomashow, L., Harsh, J., Keller, C., 2017. Molecular and microscopic insights into the formation of soil organic matter in a red pine rhizosphere. Soils 1, 4. https://doi.org/10.3390/soils1010004.

Duffy, J.E., Lefcheck, J.S., Stuart-Smith, R.D., Navarrete, S.A., Edgar, G.J., 2016. Biodiversity enhances reef fish biomass and resistance to climate change. Proceedings of the National Academy of Sciences 113, 6230–6235. https://doi.org/10.1073/pnas.1524465113.

Dutta, K., Schuur, E.A.G., Neff, J.C., Zimov, S.A., 2006. Potential carbon release from permafrost soils of Northeastern Siberia. Global Change Biology 12, 2336–2351.

Elberling, B., Michelsen, A., Schädel, C., Schuur, E.A.G., Christiansen, H.H., Berg, L., Tamstorf, M.P., Sigsgaard, C., 2013. Long-term CO2 production following permafrost thaw. Nature Climate Change 3, 890–894.

Emerson, J.B., Roux, S., Brum, J.R., Bolduc, B., Woodcroft, B.J., Jang, H. Bin, Singleton, C.M., Solden, L.M., Naas, A.E., Boyd, J.A., 2018. Host-linked soil viral ecology along a permafrost thaw gradient. Nature Microbiology 3, 870–880.

Ernakovich, J.G., Wallenstein, M.D., 2015. Permafrost microbial community traits and functional diversity indicate low activity at in situ thaw temperatures. Soil Biology and Biochemistry 87, 78–89. https://doi.org/10.1016/j.soilbio.2015.04.009.

Ernakovich, J.G., Wallenstein, M.D., Calderon, F.J., 2015. Chemical indicators of cryoturbation and microbial processing throughout an alaskan permafrost soil depth profile soil chemistry. Soil Science Society of America Journal 79, 783–793. https://doi.org/10.2136/sssaj2014.10.0420.

Ernakovich, J.G., Lynch, L.M., Brewer, P.E., Calderon, F.J., Wallenstein, M.D., 2017. Redox and temperature-sensitive changes in microbial communities and soil chemistry dictate greenhouse gas loss from thawed permafrost. Biogeochemistry. https://doi.org/10.1007/s10533-017-0354-5.

Farrell, M., Prendergast-Miller, M., Jones, D.L., Hill, P.W., Condron, L.M., 2014. Soil microbial organic nitrogen uptake is regulated by carbon availability. Soil Biology and Biochemistry 77, 261–267.

Fenner, N., Freeman, C., Reynolds, B., 2005. Observations of a seasonally shifting thermal optimum in peatland carbon-cycling processes; implications for the global carbon cycle and soil enzyme methodologies. Soil Biology and Biochemistry 37, 1814–1821.

Fontaine, S., Barot, S., Barré, P., Bdioui, N., Mary, B., Rumpel, C., 2007. Stability of organic carbon in deep soil layers controlled by fresh carbon supply. Nature 450, 277–280. https://doi.org/10.1038/nature06275.

Fox, J., Monette, G., 1992. Generalized collinearity diagnostics. Journal of the American Statistical Association 87, 178–183.

Frank-Fahle, B.A., Yergeau, É., Greer, C.W., Lantuit, H., Wagner, D., 2014. Microbial functional potential and community composition in permafrost-affected soils of the NW Canadian Arctic. PLoS One 9, e84761.

French, H.M., Slaymaker, O., 2011. Changing Cold Environments: a Canadian Perspective. John Wiley & Sons.

Frey, K.E., McClelland, J.W., 2009. Impacts of permafrost degradation on arctic river biogeochemistry. Hydrological Processes 23, 169–182. https://doi.org/10.1002/hyp.

Fujita, K., Kunito, T., Matsushita, J., Nakamura, K., Moro, H., Yoshida, S., Toda, H., Otsuka, S., Nagaoka, K., 2018. Nitrogen supply rate regulates microbial resource allocation for synthesis of nitrogen-acquiring enzymes. PLoS One 13, e0202086.

Gentsch, N., Mikutta, R., Alves, R.J.E., Barta, J., Čapek, P., Gittel, A., Hugelius, G., Kuhry, P., Lashchinskiy, N., Palmtag, J., 2015. Storage and transformation of organic matter fractions in cryoturbated permafrost soils across the Siberian Arctic. Biogeosciences 12, 4525–4542.

Gentsch, N., Wild, B., Mikutta, R., Čapek, P., Diáková, K., Schrumpf, M., Turner, S., Minnich, C., Schaarschmidt, F., Shibistova, O., 2018. Temperature response of permafrost soil carbon is attenuated by mineral protection. Global Change Biology 24, 3401–3415.

Gillespie, A.W., Sanei, H., Diochon, A., Ellert, B.H., Regier, T.Z., Chevrier, D., Dynes, J.J., Tarnocai, C., Gregorich, E.G., 2014. Perennially and annually frozen soil carbon differ in their susceptibility to decomposition: analysis of Subarctic earth hummocks by bioassay, XANES and pyrolysis. Soil Biology and Biochemistry 68, 106–116.

Gooday, G.W., 1994. Physiology of microbial degradation of chitin and chitosan. In: Biochemistry of Microbial Degradation. Springer, pp. 279–312.

Greenfield, L.M., Puissant, J., Jones, D.L., 2021. Synthesis of methods used to assess soil protease activity. Soil Biology and Biochemistry 158, 108277.

Gundelwein, A., Müller-Lupp, T., Sommerkorn, M., Haupt, E.T.K., Pfeiffer, E., Wiechmann, H., 2007. Carbon in tundra soils in the Lake Labaz region of arctic Siberia. European Journal of Soil Science 58, 1164–1174.

Haberhauer, G., Rafferty, B., Strebl, F., Gerzabek, M.H., 1998. Comparison of the composition of forest soil litter derived from three different sites at various decompositional stages using FTIR spectroscopy. Geoderma 83, 331–342.

Hemingway, J.D., Rothman, D.H., Grant, K.E., Rosengard, S.Z., Eglinton, T.I., Derry, L.A., Galy, V.V., 2019. Mineral protection regulates long-term global preservation of natural organic carbon. Nature 570, 228–231.

Herndon, E., AlBashaireh, A., Singer, D., Roy Chowdhury, T., Gu, B., Graham, D., 2017. Influence of iron redox cycling on organo-mineral associations in Arctic tundra soil. Geochimica et Cosmochimica Acta 207, 210–231. https://doi.org/10.1016/j.gca.2017.02.034.

Herndon, E., Kinsman-Costello, L., Godsey, S., 2020. Biogeochemical cycling of redox-sensitive elements in permafrost-affected ecosystems. Biogeochemical Cycles: Ecological Drivers and Environmental Impact 245–265.

Heslop, C.B., Ruess, R.W., Kielland, K., Bret-Harte, M.S., 2021. Soil enzymes illustrate the effects of alder nitrogen fixation on soil carbon processes in arctic and boreal ecosystems. Ecosphere 12, e03818.

Hess, J., Balasundaram, S.V., Bakkemo, R.I., Drula, E., Henrissat, B., Högberg, N., Eastwood, D., Skrede, I., 2021. Niche differentiation and evolution of the wood decay machinery in the invasive fungus Serpula lacrymans. The ISME Journal 15, 592–604.

Hodgkins, S.B., Tfaily, M.M., McCalley, C.K., Logan, T. a, Crill, P.M., Saleska, S.R., Rich, V.I., Chanton, J.P., 2014. Changes in peat chemistry associated with permafrost thaw increase greenhouse gas production. Proceedings of the National Academy of Sciences of the United States of America 111, 5819–5824. https://doi.org/10.1073/pnas.1314641111.

Hugelius, G., Strauss, J., Zubrzycki, S., Harden, J.W., Schuur, E.A.G., Ping, C.-L., Schirrmeister, L., Grosse, G., Michaelson, G.J., Koven, C.D., 2014. Estimated stocks of circumpolar permafrost carbon with quantified uncertainty ranges and identified data gaps. Biogeosciences 11, 6573–6593.

Hultman, J., Waldrop, M.P., Mackelprang, R., David, M.M., McFarland, J., Blazewicz, S. J., Harden, J., Turetsky, M.R., McGuire, A.D., Shah, M.B., 2015. Multi-omics of permafrost, active layer and thermokarst bog soil microbiomes. Nature 521, 208–212.

Joss, H., Patzner, M.S., Maisch, M., Mueller, C.W., Kappler, A., Bryce, C., 2022. Cryoturbation impacts iron-organic carbon associations along a permafrost soil chronosequence in northern Alaska. Geoderma 413, 115738.

Kalbitz, K., Schwesig, D., Schmerwitz, J., Kaiser, K., Haumaier, L., Glaser, B., Ellerbrock, R., Leinweber, P., 2003. Changes in properties of soil-derived dissolved organic matter induced by biodegradation. Soil Biology and Biochemistry 35, 1129–1142. https://doi.org/10.1016/S0038-0717(03)00165-2.

Kellerman, A.M., Dittmar, T., Kothawala, D.N., Tranvik, L.J., 2014. Chemodiversity of dissolved organic matter in lakes driven by climate and hydrology. Nature Communications 5, 1–8. https://doi.org/10.1038/ncomms4804.

Keuper, F., Wild, B., Kummu, M., Beer, C., Blume-Werry, G., Fontaine, S., Gavazov, K., Gentsch, N., Guggenberger, G., Hugelius, G., 2020. Carbon loss from northern circumpolar permafrost soils amplified by rhizosphere priming. Nature Geoscience 13, 560–565.

Kleber, M., 2010. What is recalcitrant soil organic matter? Environmental Chemistry 7 (4), 320–332.

Kleber, M., Bourg, I.C., Coward, E.K., Hansel, C.M., Myneni, S.C.B., Nunan, N., 2021. Dynamic interactions at the mineral–organic matter interface. Nature Reviews Earth & Environment 2, 402–421.

Knight, T.R., Dick, R.P., 2004. Differentiating microbial and stabilized β-glucosidase activity relative to soil quality. Soil Biology and Biochemistry 36, 2089–2096.

Knoblauch, C., Beer, C., Liebner, S., Grigoriev, M.N., Pfeiffer, E.-M., 2018. Methane production as key to the greenhouse gas budget of thawing permafrost. Nature Climate Change 8, 309–312.

Koven, C.D., Riley, W.J., Stern, A., 2013. Analysis of permafrost thermal dynamics and response to climate change in the CMIP5 Earth System Models. Journal of Climate 26, 1877–1900.
Koyama, A., Wallenstein, M.D., Simpson, R.T., Moore, J.C., 2013. Carbon-degrading enzyme activities stimulated by increased nutrient availability in Arctic tundra soils. PLoS One 8, 1–12. https://doi.org/10.1371/journal.pone.0077212.
Lehmann, J., Solomon, D., Kinyangi, J., Dathe, L., Wirick, S., Jacobsen, C., 2008. Spatial complexity of soil organic matter forms at nanometre scales. Nature Geoscience 1 (4), 238–242.
Levasseur, A., Drula, E., Lombard, V., Coutinho, P.M., Henrissat, B., 2013. Expansion of the enzymatic repertoire of the CAZy database to integrate auxiliary redox enzymes. Biotechnology for Biofuels 6, 1–14.
Liang, C., Schimel, J.P., Jastrow, J.D., 2017. The importance of anabolism in microbial control over soil carbon storage. Nature Microbiology 2, 17105. https://doi.org/10.1038/nmicrobiol.2017.105.
Lin, X., Handley, K.M., Gilbert, J.A., Kostka, J.E., 2015. Metabolic potential of fatty acid oxidation and anaerobic respiration by abundant members of Thaumarchaeota and Thermoplasmata in deep anoxic peat. The ISME Journal 9, 2740–2744.
Lipson, D.A., Zona, D., Raab, T.K., Bozzolo, F., Mauritz, M., Oechel, W.C., 2012. Water-table height and microtopography control biogeochemical cycling in an Arctic coastal tundra ecosystem. Biogeosciences 9 (1), 577–591.
Lynch, L.M., Machmuller, M.B., Boot, C.M., Covino, T.P., Rithner, C.D., Cotrufo, M.F., et al., 2019. Dissolved organic matter chemistry and transport along an Arctic tundra hillslope. Global Biogeochemical Cycles 33, 47–62. https://doi.org/10.1029/2018GB006030.
Lynch, L.M., Sutfin, N.A., Fegel, T.S., Boot, C.M., Covino, T.P., Wallenstein, M.D., 2019b. River channel connectivity shifts metabolite composition and dissolved organic matter chemistry. Nature Communications 10. https://doi.org/10.1038/s41467-019-08406-8.
Mackelprang, R., Waldrop, M.P., DeAngelis, K.M., David, M.M., Chavarria, K.L., Blazewicz, S.J., Rubin, E.M., Jansson, J.K., 2011. Metagenomic analysis of a permafrost microbial community reveals a rapid response to thaw. Nature 480, 368–371. https://doi.org/10.1038/nature10576.
Mackelprang, R., Burkert, A., Haw, M., Mahendrarajah, T., Conaway, C.H., Douglas, T.A., Waldrop, M.P., 2017. Microbial survival strategies in ancient permafrost: insights from metagenomics. The ISME Journal 11, 2305–2318.
Margenot, A.J., Calderón, F.J., Bowles, T.M., Parikh, S.J., Jackson, L.E., 2015. Soil organic matter functional group composition in relation to organic carbon, nitrogen, and phosphorus fractions in organically managed tomato fields. Soil Science Society of America Journal 79, 772–782.
Margenot, A.J., Calderón, F.J., Magrini, K.A., Evans, R.J., 2017a. Application of DRIFTs, 13 C NMR, and PY-MBMS to characterize the effects of soil science oxidation assays on soil organic matter composition in a Mollic Xerofluvent. Applied Spectroscopy 71, 1506–1518.
Margenot, A.J., Pulleman, M.M., Sommer, R., Paul, B.K., Parikh, S.J., Jackson, L.E., Fonte, S.J., 2017b. Biochemical proxies indicate differences in soil C cycling induced by long-term tillage and residue management in a tropical agroecosystem. Plant and Soil 420, 315–329.
Margenot, A.J., Nakayama, Y., Parikh, S.J., 2018. Methodological recommendations for optimizing assays of enzyme activities in soil samples. Soil Biology and Biochemistry 125, 350–360.
Matamala, R., Calderón, F.J., Jastrow, J.D., Fan, Z., Hofmann, S.M., Michaelson, G.J., Mishra, U., Ping, C.-L., 2017. Influence of site and soil properties on the DRIFT spectra of northern cold-region soils. Geoderma 305, 80–91.
McCalley, C.K., Woodcroft, B.J., Hodgkins, S.B., Wehr, R.A., Kim, E.-H., Mondav, R., Crill, P.M., Chanton, J.P., Rich, V.I., Tyson, G.W., 2014. Methane dynamics regulated by microbial community response to permafrost thaw. Nature 514, 478–481.
McLaren, A.D., Reshetko, L., Huber, W., 1957. Sterilization of soil by irradiation with an electron beam, and some observations on soil enzyme activity. Soil Science 83, 497–502.
McLaren, J.R., Buckeridge, K.M., van de Weg, M.J., Shaver, G.R., Schimel, J.P., Gough, L., 2017. Shrub encroachment in Arctic tundra: betula nana effects on above- and belowground litter decomposition. Ecology 98, 1361–1376. https://doi.org/10.1002/ecy.1790.
Melle, C., Wallenstein, M., Darrouzet-Nardi, A., Weintraub, M.N., 2015. Microbial activity is not always limited by nitrogen in Arctic tundra soils. Soil Biology and Biochemistry 90, 52–61. https://doi.org/10.1016/j.soilbio.2015.07.023.
Miltner, A., Bombach, P., Schmidt-Brücken, B., Kästner, M., 2012. SOM genesis: microbial biomass as a significant source. Biogeochemistry 111, 41–55. https://doi.org/10.1007/s10533-011-9658-z.
Monteux, S., Keuper, F., Fontaine, S., Gavazov, K., Hallin, S., Juhanson, J., Krab, E.J., Revaillot, S., Verbruggen, E., Walz, J., 2020. Carbon and nitrogen cycling in Yedoma permafrost controlled by microbial functional limitations. Nature Geoscience 13, 794–798.
Mori, T., Aoyagi, R., Kitayama, K., Mo, J., 2021. Does the ratio of β-1, 4-glucosidase to β-1, 4-N-acetylglucosaminidase indicate the relative resource allocation of soil microbes to C and N acquisition? Soil Biology and Biochemistry 160, 108363.
Mu, C.C., Abbott, B.W., Wu, X.D., Zhao, Q., Wang, H.J., Su, H., et al., 2017. Thaw depth determines dissolved organic carbon concentration and biodegradability on the northern Qinghai-Tibetan plateau. Geophysical Research Letters 44, 9389–9399. https://doi.org/10.1002/2017GL075067.
Nadelhoffer, K.J., Giblin, A.E., Shaver, G.R., Laundre, J.A., 1991. Effects of temperature and substrate quality on element mineralization in six arctic soils. Ecology 72, 242–253.
Nannipieri, P., Trasar-Cepeda, C., Dick, R.P., 2018. Soil enzyme activity: a brief history and biochemistry as a basis for appropriate interpretations and meta-analysis. Biology and Fertility of Soils 54, 11–19.
Nguyen, T.T., Janik, L.J., Raupach, M., 1991. Diffuse reflectance infrared Fourier transform (DRIFT) spectroscopy in soil studies. Soil Research 29, 49–67.
Nuccio, E.E., Starr, E., Karaoz, U., Brodie, E.L., Zhou, J., Tringe, S.G., Malmstrom, R.R., Woyke, T., Banfield, J.F., Firestone, M.K., 2020. Niche differentiation is spatially and temporally regulated in the rhizosphere. The ISME Journal 14, 999–1014.
Oksanen, J., Kindt, R., Legendre, P., O'Hara, B., Stevens, H.H., 2007. The Vegan Package.
Olander, L.P., Vitousek, P.M., 2000. Regulation of soil phosphatase and chitinase activityby N and P availability. Biogeochemistry 49, 175–191.
Perryman, C.R., McCalley, C.K., Ernakovich, J.G., Lamit, L.J., Shorter, J.H., Lilleskov, E., Varner, R.K., 2022. Microtopography matters Belowground CH4 cycling regulated by differing microbial processes in peatland hummocks and lawns. Journal of Geophysical Research: Biogeosciences, e2022JG006948.
Plaza, C., Pegoraro, E., Bracho, R., Celis, G., Crummer, K.G., Hutchings, J.A., Hicks Pries, C.E., Mauritz, M., Natali, S.M., Salmon, V.G., 2019. Direct observation of permafrost degradation and rapid soil carbon loss in tundra. Nature Geoscience 12, 627–631.
R Core Team, Rf, 2018. R: A Language and Environment for Statistical Computing.
Rantanen, M., Karpechko, A.Y., Lipponen, A., Nordling, K., Hyvärinen, O., Ruosteenoja, K., Vihma, T., Laaksonen, A., 2022. The Arctic has warmed nearly four times faster than the globe since 1979. Communications Earth & Environment 3, 1–10.
Romanovsky, V.E., Smith, S.L., Christiansen, H.H., 2010. Permafrost thermal state in the polar Northern Hemisphere during the international polar year 2007–2009: a synthesis. Permafrost and Periglacial Processes 21, 106–116.
Schädel, C., Schuur, E.A.G., Bracho, R., Elberling, B.O., Knoblauch, C., Lee, H., Luo, Y., Shaver, G.R., Turetsky, M.R., 2014. Circumpolar assessment of permafrost C quality and its vulnerability over time using long-term incubation data. Global Change Biology 20, 641–652.
Schaefer, K., Zhang, T., Bruhwiler, L., Barrett, A.P., 2011. Amount and timing of permafrost carbon release in response to climate warming. Tellus B: Chemical and Physical Meteorology 63, 165–180.
Schimel, J.P., Weintraub, M.N., 2003. The implications of exoenzyme activity on microbial carbon and nitrogen limitation in soil: a theoretical model. Soil Biology and Biochemistry 35, 549–563. https://doi.org/10.1016/S0038-0717(03)00015-4.
Schimel, J.P., Bilbrough, C., Welker, J.M., 2004. Increased snow depth affects microbial activity and nitrogen mineralization in two Arctic tundra communities. Soil Biology and Biochemistry 36, 217–227. https://doi.org/10.1016/j.soilbio.2003.09.008.
Schmidt, M.W.I., Torn, M.S., Abiven, S., Dittmar, T., Guggenberger, G., Janssens, I.a., Kleber, M., Kögel-Knabner, I., Lehmann, J., Manning, D.a.C., Nannipieri, P., Rasse, D.P., Weiner, S., Trumbore, S.E., 2011. Persistence of soil organic matter as an ecosystem property. Nature 478, 49–56. https://doi.org/10.1038/nature10386.
Schnecker, J., Wild, B., Hofhansl, F., Eloy Alves, R.J., Bárta, J., Čapek, P., Fuchslueger, L., Gentsch, N., Gittel, A., Guggenberger, G., 2014. Effects of soil organic matter properties and microbial community composition on enzyme activities in cryoturbated arctic soils. PLoS One 9, e94076.
Schnecker, J., Wild, B., Takriti, M., Alves, R.J.E., Gentsch, N., Gittel, A., Hofer, A., Klaus, K., Knoltsch, A., Lashchinskiy, N., 2015. Microbial community composition shapes enzyme patterns in topsoil and subsoil horizons along a latitudinal transect in Western Siberia. Soil Biology and Biochemistry 83, 106–115.
Schuur, E.A.G., Vogel, J.G., Crummer, K.G., Lee, H., Sickman, J.O., Osterkamp, T.E., 2009. The effect of permafrost thaw on old carbon release and net carbon exchange from tundra. Nature 459, 556–559. https://doi.org/10.1038/nature08031.
Seo, D.C., DeLaune, R.D., 2010. Fungal and bacterial mediated denitrification in wetlands: influence of sediment redox condition. Water Research 44, 2441–2450.
Shrotri, A., Kobayashi, H., Fukuoka, A., 2017. Catalytic conversion of structural carbohydrates and lignin to chemicals. In: Advances in Catalysis. Elsevier, pp. 59–123.
Sinsabaugh, R.L., Antibus, R.K., Linkins, A.E., McClaugherty, C.A., Rayburn, L., Repert, D., Weiland, T., 1993. Wood decomposition: nitrogen and phosphorus dynamics in relation to extracellular enzyme activity. Ecology 74, 1586–1593.
Sinsabaugh, R.L., Turner, B.L., Talbot, J.M., Waring, B.G., Powers, J.S., Kuske, C.R., Moorhead, D.L., Follstad Shah, J.J., 2016. Stoichiometry of microbial carbon use efficiency in soils. Ecological Monographs 86, 172–189.
Sistla, S.A., Schimel, J.P., 2013. Seasonal patterns of microbial extracellular enzyme activities in an arctic tundra soil: identifying direct and indirect effects of long-term summer warming. Soil Biology and Biochemistry 66, 119–129.
Sjögersten, S., Caul, S., Daniell, T.J., Jurd, A.P.S., O'Sullivan, O.S., Stapleton, C.S., Titman, J.J., 2016. Organic matter chemistry controls greenhouse gas emissions from permafrost peatlands. Soil Biology and Biochemistry 98, 42–53.
Skujins, J.J., 1967. Enzymes in soil. Soil Biochemistry 1, 371–414.
Slater, A.G., Lawrence, D.M., 2013. Diagnosing present and future permafrost from climate models. Journal of Climate 26, 5608–5623.
Smith, S.L., O'Neill, H.B., Isaksen, K., Noetzli, J., Romanovsky, V.E., 2022. The changing thermal state of permafrost. Nature Reviews Earth & Environment 3, 10–23.
Sokol, N.W., Bradford, M.A., 2019. Microbial formation of stable soil carbon is more efficient from belowground than aboveground input. Nature Geoscience 12, 46–53.
Spohn, M., Kuzyakov, Y., 2013. Phosphorus mineralization can be driven by microbial need for carbon. Soil Biology and Biochemistry 61, 69–75.
Steenbergh, A.K., Bodelier, P.L.E., Hoogveld, H.L., Slomp, C.P., Laanbroek, H.J., 2011. Phosphatases relieve carbon limitation of microbial activity in Baltic Sea sediments along a redox-gradient. Limnology & Oceanography 56, 2018–2026.

Strauss, J., Biasi, C., Sanders, T., Abbott, B.W., von Deimling, T.S., Voigt, C., Winkel, M., Marushchak, M.E., Kou, D., Fuchs, M., 2022. A globally relevant stock of soil nitrogen in the Yedoma permafrost domain. Nature Communications 13, 1–9.

Sturm, M., Racine, C., Tape, K., 2001. Climate change. Increasing shrub abundance in the Arctic. Nature 411, 546–547. https://doi.org/10.1038/35079180.

Sturm, M., Schimel, J.P., Michaelson, G., Welker, J.M., Oberbauer, S.F., Liston, G.E., Fahnestock, J., Romanovsky, V.E., 2005. Winter biological processes could help convert arctic tundra to shrubland. BioScience 55, 17–26. https://doi.org/10.2307/1294386.

Swenson, T.L., Bowen, B.P., Nico, P.S., Northen, T.R., 2015. Competitive sorption of microbial metabolites on an iron oxide mineral. Soil Biology and Biochemistry 90, 34–41. https://doi.org/10.1016/j.soilbio.2015.07.022.

Tank, S.E., Fellman, J.B., Hood, E., Kritzberg, E.S., 2018. Beyond respiration: controls on lateral carbon fluxes across the terrestrial-aquatic interface. Limnology and Oceanography Letters 3, 76–88.

Tank, S.E., Vonk, J.E., Walvoord, M.A., McClelland, J.W., Laurion, I., Abbott, B.W., 2020. Landscape matters: predicting the biogeochemical effects of permafrost thaw on aquatic networks with a state factor approach. Permafrost and Periglacial Processes 31, 358–370.

Tarnocai, C., Smith, C., 1993. The formation and properties of soils in the permafrost regions of Canada. In: Gilichinsky, D.A. (Ed.), Proc. First Internat. Conf. On Cryopedology. Russia Academy of Sciences, pp. 21–42. Pushchino.

Taş, N., Prestat, E., Wang, S., Wu, Y., Ulrich, C., Kneafsey, T., Tringe, S.G., Torn, M.S., Hubbard, S.S., Jansson, J.K., 2018. Landscape topography structures the soil microbiome in arctic polygonal tundra. Nature Communications 9, 1–13.

Tian, P., Razavi, B.S., Zhang, X., Wang, Q., Blagodatskaya, E., 2020. Microbial growth and enzyme kinetics in rhizosphere hotspots are modulated by soil organics and nutrient availability. Soil Biology and Biochemistry 141, 107662.

Trivedi, P., Delgado-Baquerizo, M., Trivedi, C., Hu, H., Anderson, I.C., Jeffries, T.C., Zhou, J., Singh, B.K., 2016. Microbial regulation of the soil carbon cycle: evidence from gene–enzyme relationships. The ISME Journal 10, 2593–2604.

Vogel, C., Mueller, C.W., Hoschen, C., Buegger, F., Heister, K., Schulz, S., Schloter, M., Kogel-Knabner, I., 2014. Submicron structures provide preferential spots for carbon and nitrogen sequestration in soils. Nature Communications 5, 1–7. https://doi.org/10.1038/ncomms3947.

Von Freyberg, J., Radny, D., Gall, H.E., Schirmer, M., 2014. Implications of hydrologic connectivity between hillslopes and riparian zones on streamflow composition. Journal of Contaminant Hydrology 169, 62–74. https://doi.org/10.1016/j.jconhyd.2014.07.005.

Wallenstein, M.D., McMahon, S.K., Schimel, J.P., 2009. Seasonal variation in enzyme activities and temperature sensitivities in Arctic tundra soils. Global Change Biology 15, 1631–1639. https://doi.org/10.1111/j.1365-2486.2008.01819.x.

Wallenstein, M., Allison, S.D., Ernakovich, J., Steinweg, J.M., Sinsabaugh, R., 2010. Controls on the temperature sensitivity of soil enzymes: a key driver of in situ enzyme activity rates. In: Soil Enzymology. Springer, pp. 245–258.

Walz, J., Knoblauch, C., Böhme, L., Pfeiffer, E.-M., 2017. Regulation of soil organic matter decomposition in permafrost-affected Siberian tundra soils-Impact of oxygen availability, freezing and thawing, temperature, and labile organic matter. Soil Biology and Biochemistry 110, 34–43.

Wang, J., Wu, Y., Zhou, J., Bing, H., Sun, H., 2016. Carbon demand drives microbial mineralization of organic phosphorus during the early stage of soil development. Biology and Fertility of Soils 52, 825–839.

Wang, Y., Wang, H., He, J.-S., Feng, X., 2017. Iron-mediated soil carbon response to water-table decline in an alpine wetland. Nature Communications 8, 1–9.

Wang, Y., Xu, Y., Wei, D., Shi, L., Jia, Z., Yang, Y., 2020. Different chemical composition and storage mechanism of soil organic matter between active and permafrost layers on the Qinghai–Tibetan Plateau. Journal of Soils and Sediments 20, 653–664.

Ward, C.P., Cory, R.M., 2015. Chemical composition of dissolved organic matter draining permafrost soils. Geochimica et Cosmochimica Acta 167, 63–79. https://doi.org/10.1016/j.gca.2015.07.001.

Weedon, T., Kowalchuk, J.A., G Aerts, R., van Hal, J., van Logtestijn, R., Taş, N., Fm Röling, W., M. van Bodegom, P., 2012. Summer warming accelerates sub-arctic peatland nitrogen cycling without changing enzyme pools or microbial community structure. Global Change Biology 18, 138–150.

Wild, B., Schnecker, J., Alves, R.J.E., Barsukov, P., Barta, J., Capek, P., Gentsch, N., Gittel, A., Guggenberger, G., Lashchinskiy, N., Mikutta, R., 2014. Input of easily available organic C and N stimulates microbial decomposition of soil organic matter in arctic permafrost soil. Soil Biology and Biochemistry 75, 143–151. https://doi.org/10.1016/j.soilbio.2014.04.014.

Wild, B., Gentsch, N., Čapek, P., Diáková, K., Alves, R.J.E., Bárta, J., Gittel, A., Hugelius, G., Knoltsch, A., Kuhry, P., 2016. Plant-derived compounds stimulate the decomposition of organic matter in arctic permafrost soils. Scientific Reports 6, 1–11.

Woods, G.C., Simpson, M.J., Pautler, B.G., Lamoureux, S.F., Lafrenière, M.J., Simpson, A.J., 2011. Evidence for the enhanced lability of dissolved organic matter following permafrost slope disturbance in the Canadian High Arctic. Geochimica et Cosmochimica Acta 75 (22), 7226–7241.

Zeglin, L.H., Stursova, M., Sinsabaugh, R.L., Collins, S.L., 2007. Microbial responses to nitrogen addition in three contrasting grassland ecosystems. Oecologia 154, 349–359.

Zhang, T., Barry, R.G., Knowles, K., Heginbottom, J.A., Brown, J., 1999. Statistics and characteristics of permafrost and ground-ice distribution in the Northern Hemisphere. Polar Geography 23, 132–154.

Zhang, X., Hutchings, J.A., Bianchi, T.S., Liu, Y., Arellano, A.R., Schuur, E.A.G., 2017. Importance of lateral flux and its percolation depth on organic carbon export in Arctic tundra soil: implications from a soil leaching experiment. Journal of Geophysical Research: Biogeosciences 122, 796–810. https://doi.org/10.1002/2016JG003754.

Zhou, L., Zhou, Y., Yao, X., Cai, J., Liu, X., Tang, X., Zhang, Y., Jang, K.-S., Jeppesen, E., 2020. Decreasing diversity of rare bacterial subcommunities relates to dissolved organic matter along permafrost thawing gradients. Environment International 134.

Zuppinger-Dingley, D., Schmid, B., Petermann, J.S., Yadav, V., De Deyn, G.B., Flynn, D.F.B., 2014. Selection for niche differentiation in plant communities increases biodiversity effects. Nature 515, 108–111.

Zuur, A.F., Ieno, E.N., Walker, N.J., Saveliev, A.A., Smith, G.M., 2009. Mixed Effects Models and Extensions in Ecology with R. Springer.

Zuur, A.F., Ieno, E.N., Elphick, C.S., 2010. A protocol for data exploration to avoid common statistical problems. Methods in Ecology and Evolution 1, 3–14. https://doi.org/10.1111/j.2041-210X.2009.00001.x.